# 3D Fluid dynamic analyses of open joint ventilated facades applying experimental Stereo-PIV techniques.

M. Nuria Sánchez [*1], Cristina Sanjuan [1] and M. Rosario Heras [1]

*1 Department of Energy, Energy Efficiency in Buildings Unit, CIEMAT*
*Av. Complutense, 40. Madrid 28040, Spain*
**Corresponding author: nuria.sanchez@ciemat.es*

## ABSTRACT

Open joint ventilated façade (OJVF) is a passive constructive system widely used to ameliorate envelop of buildings, improving their energy efficiency. A laboratory model of a ventilated façade with horizontal and vertical open joints was used to study thermal and fluid-dynamic behaviour of this system. Experimental Stereo Particle Image Velocimetry (Stereo-PIV 2D-3C) was applied to study the fluid dynamic performance of this model. In addition, thermal analyses were performed applying infrared thermography and air temperature monitoring inside the ventilated cavity. Experimental measurements were carried out inside the air cavity in a vertical joint plane and in a middle plane of panels, corresponding to horizontal joints. Radiation condition corresponds to $1x10^9$ Ra and wind effect is not considered.
The analysis of the data confirms previous results of velocity and temperature patterns for OJVF with horizontal joints and leads to identify two different velocity patterns corresponding to the airflow entrance through horizontal and vertical joints. Experimental results will be used for validate computational fluid dynamics (CFD) models of the OJVF system.

## KEYWORDS

Ventilated facade; natural convection; Stereo-PIV.

## 1 INTRODUCTION

The four major energy end-use sectors are commercial, residential, industrial and transportation. Commercial and residential buildings account for over 40% of total final energy consumption (EIA, 2014), representing cooling loads an important percentage of it. To reduce energy consumption in this sector, a combination of best available technologies and public policies has to be adopted.
Different passive systems are implemented in the built environment for enhancement of sustainability, achieving the goal of saving energy while maintaining thermal comfort conditions (GhaffarianHoseini et al., 2012 and Romila et al., 2012).
A commonly used system are Open joint ventilated façades (OJVF), reducing the heat transferred to the building and consequently the cooling loads. The solar radiation incident on the external surface of the OJVF produces an ascending airflow, induced by the buoyancy effect, which extracts part of the heat to the ambient air.
The system, composed by multiple layers, is characterized by an external opaque coating and a ventilated air cavity formed between the envelope and the insulation layer attached to outer side of the wall mass (Figure 1). The exterior coat is made of tiles hanged to the structure forming open joints between them, horizontally or vertically oriented.

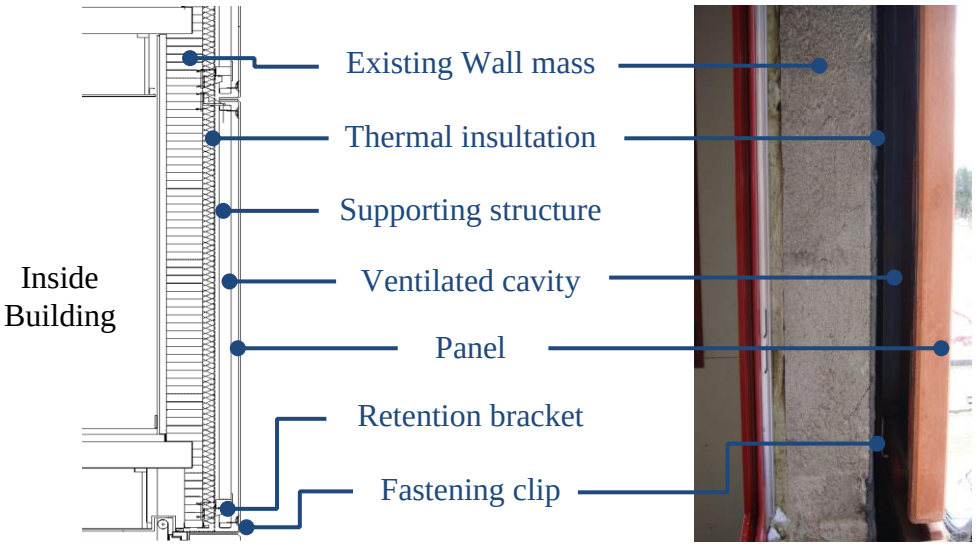


Figure 1: From left to right: open joint ventilated façade design and image of the component installation during building refurbishment.

Several authors assess experimentally the effect on the performance of the system of different constructive parameters: height of the ventilated camara, facade orientation, environmental conditions or material of panels (Marinosci et al., 2014 and Stazi et al., 2014). Moreover, several studies evaluate the performance of OJVF with horizontal joints based on 2D-PIV, a non-intrusive particle based technique used in flow velocity measurement (Sánchez et al., 2013 and Sanjuan et al., 2011 and 2012). This optical method of flow visualization and quantification of instantaneous velocity fields, measures two velocity components in the area of analysis. The measurement principles and technology description have been reviewed by Cao et al., (2014) dealing with the applications in indoor environment. The current research is focused on analyse the thermal and energy behaviour of OJVF with vertical and horizontal open joints, determining the role of orientation in the performance of the component.

## 2 EXPERIMENTAL SETUP

### 2.1 Model Design

An experimental model of a ventilated façade with horizontal and vertical open joints was designed and constructed to ensure the natural ventilation flow simulation in analogous conditions to real façades. In this model, the exterior coat is made up of 16 metallic panels disposed in a symmetrical distribution of 4 rows and 4 columns with 5 mm horizontal and vertical open joints (Figure 2).

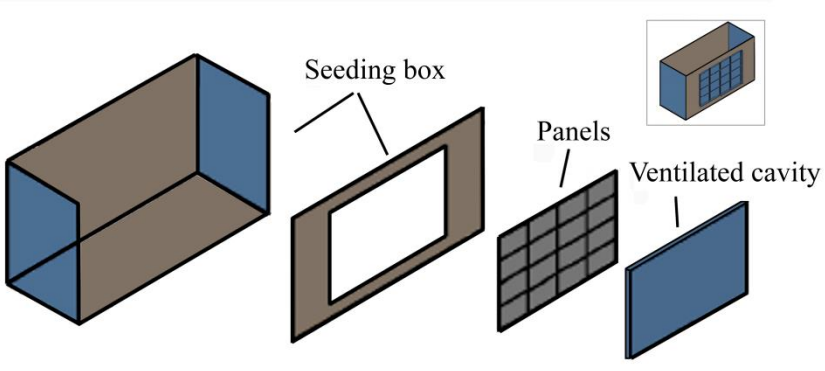


Figure 2: Exploded diagram of the experimental model of a ventilated façade with horizontal and vertical open joints.

Overall dimensions of the facade were 0.825 m high and 1.225 m wide with a ventilated cavity of 0.045 m. Additionally, a seeding box was rigidly attached to the ventilated facade on its outer surface, simulating the outdoor environment.
The design is based on simplified real facades required for experiments in the laboratory setting. The dimensions of the cavity and the joints correspond to real façades dimensions while the height of the model has been reduced to a third of the distance between window panes in real buildings. Moreover, thermal insulation and wall mass layers were replaced by a glass layer to allow optical access to the ventilated cavity. These limitations are mainly due to the height of the laboratory and the specific requirements of the experimental technique used for the characterization of the ventilation flow.
The natural ventilation airflow inside the camera was induced by heating the external surface of the panels using auto-adhesive electrical heater mats; simulating the solar radiation effect.

### 2.2 Experimental measurement techniques

Particle Image Velocimetry measures instantaneous flow fields capturing two images shortly, one after each other. Statistical correlations are used to find average tracer particle displacement (illuminated by a sheet of light) within this time. From the known time difference and the measured displacement, the instantaneous velocity field is calculated. Stereo-PIV (2D3C) unlike PIV (2D2C) uses two points of view (two cameras) and images are recorded simultaneously by left and right cameras. A numerical model describing how objects in 3-dimensional space are mapped onto the 2-dimensional image (recorded by each of the cameras) is used to estimate the third velocity component in the area of analysis (Hinsch, 1995).
The Stereo-PIV technique was applied to study the fluid dynamic performance of the constructed OJVF model. The three velocity components of the ventilation airflow were measured, obtaining the instantaneous velocity field. A rotation configuration arrangement with cameras on either side of this plane was performed. In order to achieve a maximal overlap of the area covered by both cameras in the stereoscopic PIV 3D-reconstruction, viewing angles of the cameras were set to 45º. The true 3D displacement (ΔX, ΔY,ΔZ) is estimated from a pair of 2D displacements (Δx,Δy) as seen from left and right camera respectively (Figure 3).

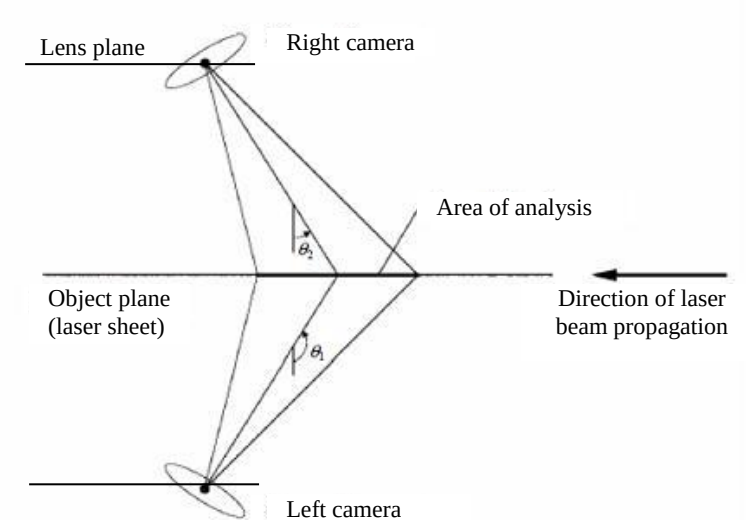


Figure 3: Schematic of the angular displacement system in Stereo-PIV.

One micron olive oil droplets were used as tracer particles; introduced into the air inside the seeding box. The image density was larger than 15 particles and air flow was homogeneously

seeding. The value of the Stokes numbers for the experiments is in the range of $10^{-6}$ indicating that the particles follow the fluid flow.
Vertical dimension of the active area of the cameras was almost one order of magnitude lower than the cavity height (15cm compared with 82cm). As a result, the experimental device was eight times vertically displaced 10cm up to the maximum height of the air cavity.
Measurements registered at the eight different runs were reconstructed, obtaining the whole velocity field in vertical plane. 250 snapshots were recorded for each run with a frequency of 17 Hz. The time between pulses was $10^{-4}$ s.
A correct calibration is an essential prerequisite for measuring accurately the three velocity components. Thus, Stereo Automapping was applied in order to correct the misalignment between calibration plate and laser light sheet, resulting one of the major sources of error in Stereo-PIV. This self-calibration procedure computes the cross-correlation and disparity map between images of left and right camera recorded at the same time.
Image processing was done using multi-grid algorithm with 64x64 pixel initial window size and 32x32 pixel final window size with an overlap of 50%. At a later stage, spurious vectors were eliminated from the flow field in the post-processing.
In addition, thermal analyses were performed applying infrared thermography and air temperature monitoring. The temperature measurements were performed using an infrared thermograph camera and thermocouple sensors, respectively.
Both, temperature and velocity measurements, were obtained in two different vertical planes of the air cavity, corresponding to a middle plane characterized by the horizontal joints and a vertical joint plane.

## 3 RESULTS

This research is conducted considering solar radiation corresponding to $1x10^9$ Rayleigh and without considering the wind effect. Relevant thermal experimental conditions are: the heater mats powered by 10 V dc within a power rating of 28W simulating an absorbed solar radiation of 460W/m2, the 51ºC mean temperature of slabs, the 29ºC seeding temperature and the calculated Stokes number of $1.01x10^9$.

### 3.1 Mean Velocity Field

Based on real-time field velocity, it is possible to calculate other factors involved in fluid dynamics such as average velocity field. Instantaneous velocity can be regarded as consisting of an average value u indicated by the dashed line, plus a random fluctuation $u_i$' (Equation 1).

$$u_i(x,y,z) = \bar{u}(x,y,z) + u_i'(x,y,z) \quad (1)$$

For computing the averaged velocity vector fields, only vectors from snapshots with time correlation factors higher that 99% were used in the mean flow calculation.
Figure 4 shows time-averaged velocity field in a middle-panel plane of measurement at three different cavity heights (bottom, middle and top). Similarly, Figure 5 shows time-averaged velocity field in a joint plane of measurement at three different cavity heights (bottom, middle and top). Maximum time-averaged velocity field was 0.35m/s, at the bottom of the air cavity in the joint plane.
Significantly, two different patterns were identified for the same Rayleigh value, corresponding to the airflow entrance through horizontal and vertical joints. Figure 4 and Figure 5 shows these two patterns especially at the bottom of the cavity. In both patterns the air enters the ventilated cavity through the lower open joints and leaves it through the upper joints. At half height of the air cavity, the pressure equilibrium prevents the exterior air not enter or leave the cavity through the joints.

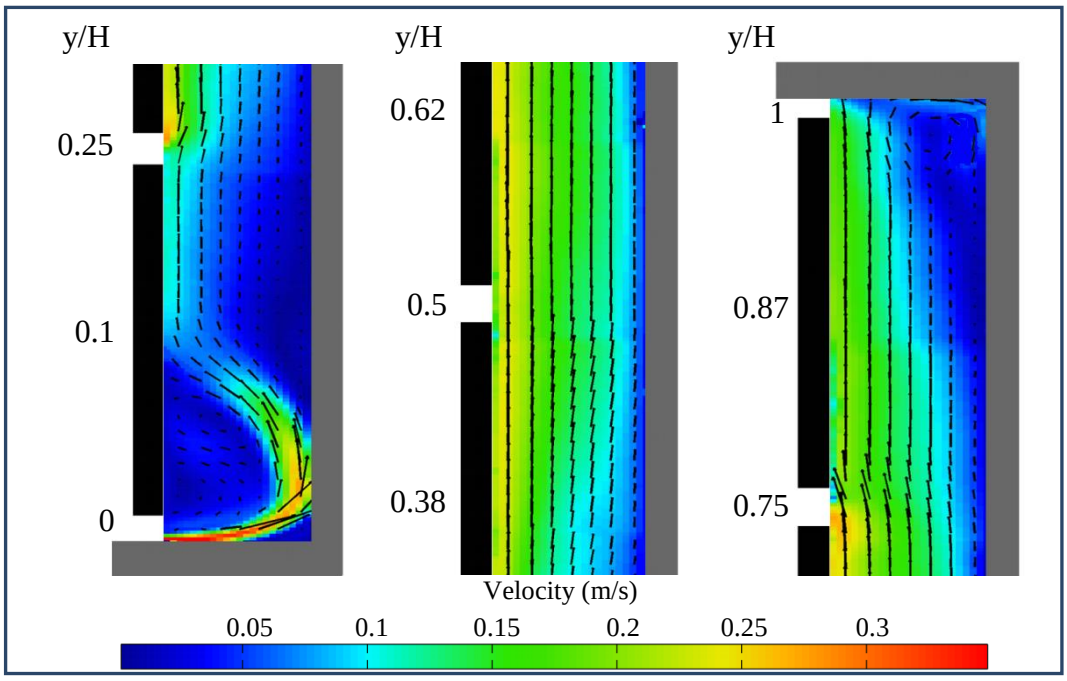


Figure 4: From left to right: time-averaged velocity field in a middle plane of measurement at three different cavity heights.

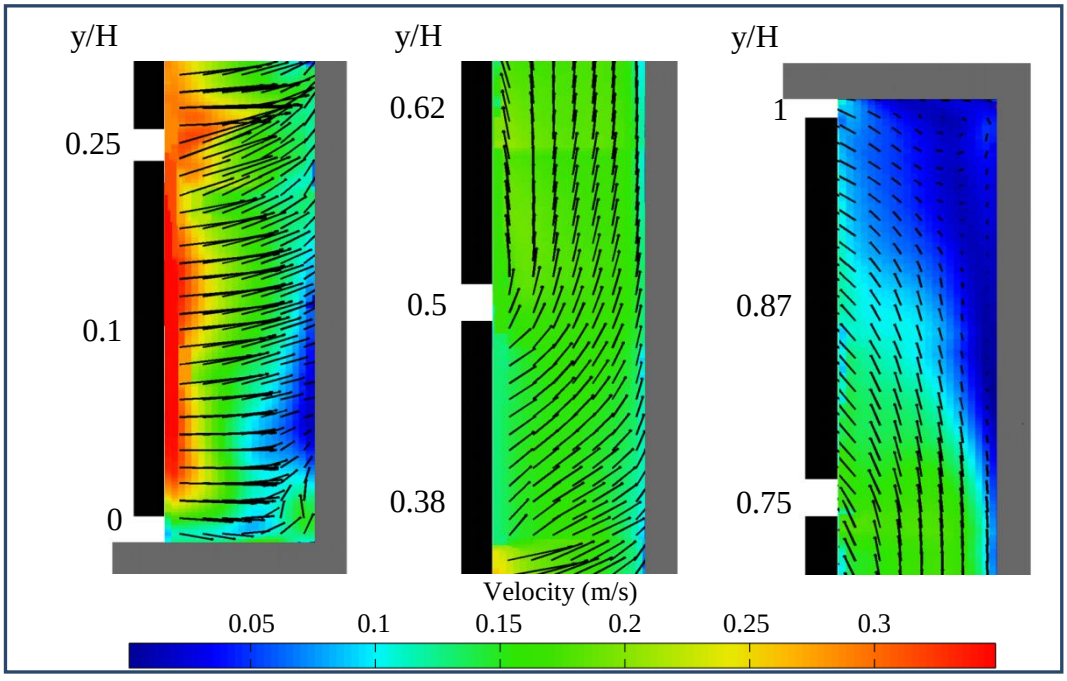


Figure 5: From left to right: time-averaged velocity field in a joint plane of measurement at three different cavity heights.

The buoyancy effect created inside the air cavity by heating the external surface of the panels produces an ascending ventilation flow that circulates along the cavity at an inhomogeneous rate. The abrupt entrance of the airflow through the lower horizontal joints generates recirculation vortexes (Figure 4); complex fluid structures due to the presence of slabs along the wall. However no recirculation vortexes were identified at the lower vertical joints because the fluid enters the cavity without interruption throughout the open vertical joints (Figure 5).

### 3.2 Turbulence

Derived magnitudes from velocity such as turbulence were calculated to further characterize the air movement inside the cavity (Equation 2).

$$Tu(x,y,z) = \sqrt{\frac{2}{3}K(x,y,z)} \tag{2}$$

Kinetic energy corresponding to the random velocity component is referred to as turbulence kinetic energy (K) and calculated by the following equation (Equation 3).

$$K(x,y,z) = \frac{1}{2N}\sum_{i=1}^{N}[u_i'^2(x,y,z) + v_i'^2(x,y,z) + w_i'^2(x,y,z)] \tag{3}$$

N is the number of snapshots.

Figure 6 shows turbulence level in a middle-panel plane of measurement at three different cavity heights (bottom, middle and top). Similarly, Figure 7 shows turbulence level in a joint plane of measurement at three different cavity heights (bottom, middle and top).

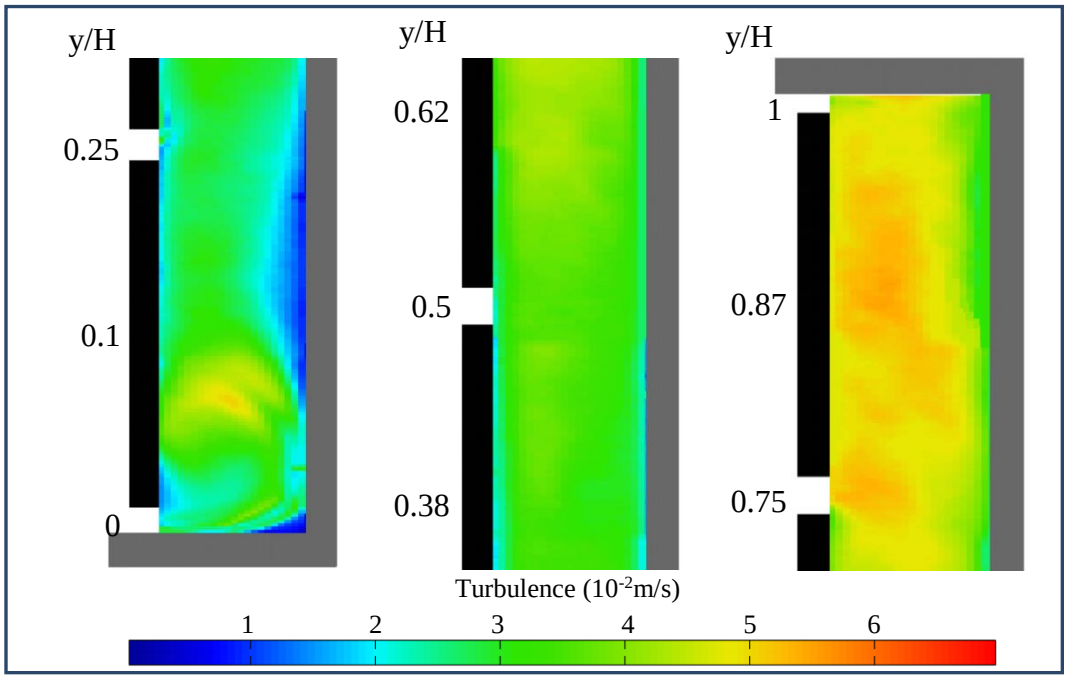


Figure 6: From left to right: turbulence in a middle plane of measurement at three different cavity heights.

As it would be expected, the turbulence level increases with the mean flow velocity, quantifying the oscillation part of the velocity. Maximum turbulence level was 0.07 m/s, determined at the bottom of the air cavity in the joint plane.

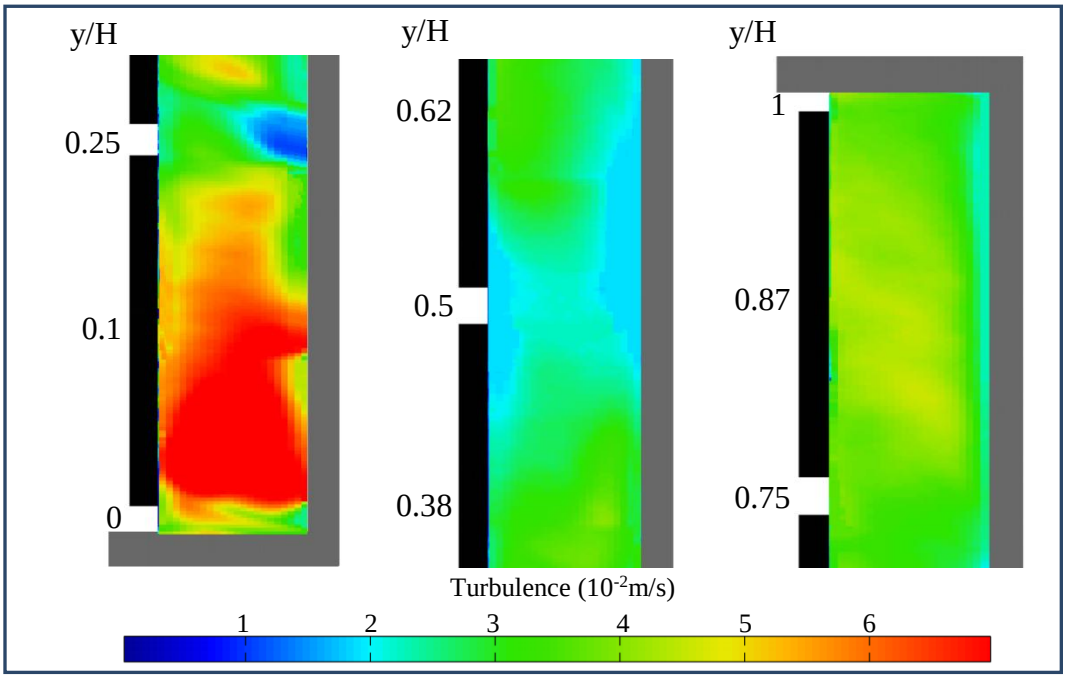


Figure 7: From left to right: turbulence in a joint plane of measurement at three different cavity heights.

### 3.3 Temperature measurements

Simultaneously to the performance of the Stereo-PIV experiments, the OJVF model was monitored measuring the temperatures in the outer surface, the interior air cavity, and the environmental conditions. Figure 8 represents summarized time-averaged temperatures measured during the experiments corresponding to the two vertical planes (middle-panel plane and joint plane).

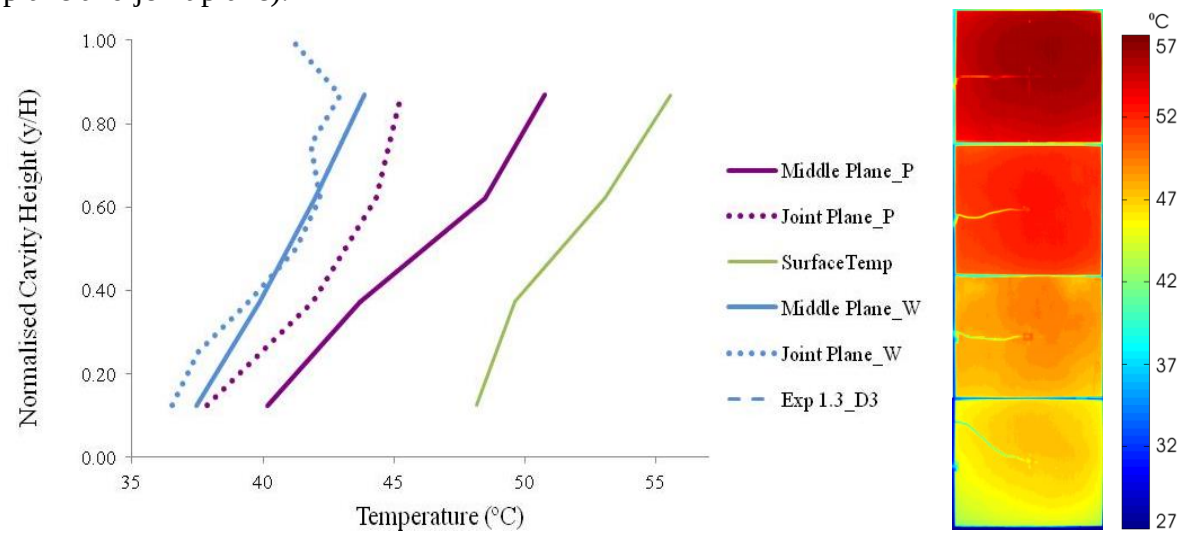


Figure 8: From left to right: air temperature at the centre of the ventilated cavity and surface temperature of the panels.

The temperatures monitored close to the entrance of the channel shows higher values of the air temperature at the middle plane compared to the joint plane. The temperatures monitored close to the wall mass of the channel show similar values of the air temperature at the middle plane and the joint plane The surface temperature at the centre of the panels ranged from 48ºC to 56ºC.

Additional measurements include infrared thermography in selected monitored panels. The surface temperature registered with a thermographic camera also shows higher temperature values at the centre of the plates according to the previous measurements. The distribution of superficial temperature in the panels is not homogeneous. Temperature values are lower near the edges due to the ventilation airflow through the joints.

## 4 CONCLUSIONS

This study concludes that airflow inside the cavity can be considered as a steady turbulent flow. Two different patterns were identified corresponding to the airflow entrance through horizontal and vertical joints with a maximum time-averaged velocity field of 0.35m/s. The evolution of the velocity profiles along the cavity was different. In both patterns the air enters the ventilated cavity through the lower open joints and leaves it through the upper joints. The abrupt entrance of the airflow through the lower horizontal joints generates recirculation vortexes. However, the evolution of the velocity profiles along the cavity was different.
The temperatures monitoring shows higher values of the air temperature at the middle plane compared to the joint plane. The air temperature increased due to the heat exchange of the panels and the ventilated cavity walls with the ascending flow. The surface temperature registered with a thermographic camera shows higher temperature values at the upper panels and higher temperature values at the centre of the panels.
The fluid pattern corresponding to the middle plane (horizontal joint) reproduces well the previous studies (Sánchez et al., 2013 and Sanjuan et al., 2011).
These experimental results help to validate CFD models to predict accurately the heat transferred to the building. Besides, additional studies considering different radiation conditions and several relevant constructive parameters have to be done.

## 5 ACKNOWLEDGEMENTS

This work has been developed in the framework of the OMEGA-CM programme and the experimental facility was initially developed under the PSE-ARFRISOL project. The OMEGA-CM programme, ref. P2013/MAE2835, is a multidisciplinary R&D programme supported by the Madrid Regional Government and co-financed by EU Structural Funds. The PSE-ARFRISOL, ref. PSE-120000-2005-1, is a scientific-technical research project of singular character, supported by the Spanish Ministry of Science and Innovation and co-financed by FEDER funds. The authors thank OMEGA-CM and ARFRISOL members.

## 6 REFERENCES

EIA. (2014). Independent Statistics and Analysis U.S. Energy Information Administration. www.eia.gov (Access June 2015).

GhaffarianHoseini A.H., Berardi U., Ali GhaffarianHoseini A. and Makaremi N. (2012). Intelligent Facades in Low-Energy Buildings. *British Journal of Environment and Climate Change*, 2(4), 437-464.

Romila C., Popovici C.G., Cherecheş N.C. (2012). Reduction of building energy consumption using ventilated façades. *Environmental Engineering and Management Journal*, 11(4), 806-811.

Marinosci C., Semprini G., Morini G.L. (2014). Experimental analysis of the summer thermal performances of a naturally ventilated rainscreen façade building. *Energy and Buildings*, 72, 280–287.

Stazi F., Veglìoa A., Di Perna C. (2014). Experimental assessment of a zinc-titanium ventilated fac¸ ade in a Mediterranean climate. *Energy and Buildings*, 69, 525–534.

Sánchez M.N., Sanjuan C., Suárez M.J., Heras M.R. (2013). Experimental assessment of the performance of open joint ventilated façades with buoyancy-driven airflow. *Solar Energy*, 91, 131-144.

Sanjuan C., Sánchez M.N., Heras M.R., Blanco E. (2011). Experimental analysis of natural convection in open joint ventilated façades with 2D PIV. *Building & Environment*, 46(11), 2314-2325.

Sanjuan C., Sánchez M.N., Enríquez R., Heras M.R. (2012). Experimental PIV techniques applied to the analysis of natural convection in open joint ventilated facades. *Energy Procedia*, 30, 1216-1225.

Cao, X., Liu, J., Jiang, N., Chen, Q. (2014). Particle image velocimetry measurement of indoor airflow field: A review of the technologies and applications. *Energy and Buildings*, 69, 367-380.

Hinsch, K.D. (1995) Three-dimensional particle velocimetry. *Meas. Sci. Technol.*, 6, 742-753.